

**COMPUTERIZED BREAST CANCER DIAGNOSIS
AND PROGNOSIS FROM FINE NEEDLE ASPIRATES**

William H. Wolberg, M.D., W. Nick Street, Ph.D., Dennis M.
Heisey, Ph.D., Olvi L. Mangasarian, Ph.D.

Departments of Surgery, Human Oncology, and Computer Sciences
University of Wisconsin, Madison, WI

Dr. Wolberg is Professor of Surgery and Human Oncology,
University of Wisconsin, Madison, WI

Dr. Street is Assistant Researcher in the Departments of Surgery
and Computer Sciences, University of Wisconsin, Madison, WI

Dr. Heisey is Assistant Scientist in the Department of Surgery,
University of Wisconsin, Madison, WI

Dr. Mangasarian is John von Neumann Professor of Mathematics and
Computer Sciences, University of Wisconsin, Madison, WI

Corresponding author and address for reprints:

William H. Wolberg, M.D.

Department of Surgery, 600 Highland Avenue, Madison, WI
53792

FAX 608 263 7652, Phone 608 263 8604

This paper was presented at the Western Surgical Association
meeting in Palm Desert, California, November 14, 1994.

This study was supported in part by Air Force Office of Scientific Research grant AFOSR F49620-94-1-0036 and National Science Foundation grant CCR-9101801.

ABSTRACT:

Objectives: Use digital image analysis and machine-learning to:
1) improve breast mass diagnosis based on fine needle aspirates (FNA), and 2) improve breast cancer prognostic estimations.

Design: An interactive computer system evaluates, diagnoses, and determines prognosis based on cytologic features derived directly from a digital scan of fine-needle aspirate slides.

Setting: The University of Wisconsin (Madison) Departments of Computer Science and Surgery, and the University of Wisconsin Hospital and Clinics, a university teaching hospital.

Patients: Five hundred sixty-nine consecutive patients (212 with cancer, 357 with benign masses) provided the data for the diagnostic algorithm, and an additional 118 (31 with malignant masses and 87 with benign masses) consecutive, new patients tested the algorithm. 190 of these patients with invasive cancer and without distant metastases were used for prognosis.

Interventions: Surgical biopsy specimens were taken from all cancers and some benign masses. The remaining cytologically benign masses were followed up for a year and surgical biopsy specimens were taken if they changed in size or character. Patients with cancer received standard treatment.

Outcome Measures: Cross validation was used to project the accuracy of the diagnostic algorithm and to determine the importance of prognostic features. In addition, the mean errors were calculated between the actual times of distant disease occurrence and the times predicted using various prognostic features. Statistical analyses were also done.

Results: The predicted diagnostic accuracy was 97% and the actual diagnostic accuracy on 118 new samples was 100%. Tumor size and lymph node status were weak prognosticators compared with nuclear features, in particular those measuring nuclear size. Compared with the actual time for recurrence, the mean error of predicted times for recurrence with the nuclear features was 17.9 months and was 20.1 months with tumor size and lymph node status ($p=0.11$).

Conclusions: Computer technology will improve breast fine-needle aspiration accuracy and prognostic estimations.

New methods were developed for this research. First, we developed image analysis methods to quantitate nuclear features, and second, we developed machine learning methods based on linear programming that were applicable to breast cancer diagnosis and prognostic estimation. We used these methods to 1) improve breast mass diagnosis based on fine needle aspirates (FNA), and 2) improve breast cancer prognostic estimations.

The diagnostic accuracy of FNA to diagnose breast masses is so operator dependent that some recommend the development of individual performance characteristics for persons doing the test¹. The reported accuracy of visually diagnosed breast FNAs is more than 90%², but the accuracy achieved in individual series varies considerably, reflecting the subjectivity of the procedure. In addition, it is unlikely that such reported accuracy is generally achieved because the bias is toward publishing favorable results. Visually assessed size, shape, and texture features that distinguish benign from malignant cells and that are prognostically important are now measured by computers. This computer technology avoids the inherent subjectivity of visual interpretation. Once nuclear features are quantitated, machine learning techniques³ are used to make a diagnosis and to estimate prognosis.

Materials and Methods

Patients and Aspirate

The benign and malignant cell samples used in this study

were obtained by FNA from a consecutive series of 569 patients: 212 with cancer and 357 with fibrocystic breast masses. An additional 118 (31 malignant and 87 benign) consecutive, new patients tested the diagnostic algorithm. Prognostic models for distant metastases were developed from the 190 cancer patients with invasive cancer who did not have evident distant metastases at diagnosis.

FNAs were expressed onto a silane-prepared glass slide, a similar slide was placed face to face and the slides were separated with a horizontal motion. Preparations are immediately fixed in 95% ethanol, stained with hematoxylin and eosin, and processed.

In our analysis, aspirates were classified as cancer based on surgical biopsy and histologic confirmation. Cytologically diagnosed benign breast masses were confirmed either by biopsy or by follow-up for a year. After a year, non-biopsied masses were considered to be benign if they had not enlarged ⁴.

Image Preparation

The imaged area on the aspirate slides was visually selected for minimal nuclear overlap. The image for digital analysis was generated by a JVC TK-1070U color video camera mounted atop an Olympus microscope and the image was projected into the camera with a 63 X objective and a 2.5 X ocular. The image was captured by a ComputerEyes/RT color framegrabber board (Digital Vision, Inc., Dedham MA) as a 640 x 400, 8-bit-per-pixel Targa file.

The User Interface (Xcyt)

A graphical computer program called Xcyt was developed that allows the user to input the approximate location of a sufficient number of nuclei (10 to 20) to provide a representative sample.

A mouse was used to trace a rough outline of cell nuclei on the computer monitor. From this rough outline, the actual boundary of the cell nucleus was located by an active contour model known as a "snake"^{5,6}. The mathematical aspects of the snake calculations are described elsewhere³.

Nuclear Features

Once the nuclei to be analyzed have been identified by the operator and have been enclosed by the computer-generated snakes, the computer calculates ten nuclear features for each nucleus. These features are modeled such that higher values are typically associated with malignancy. Features were verified using idealized phantom cells². Nuclear size is expressed by the Radius and Area features. Nuclear shape is expressed by Smoothness, Concavity, Compactness, Concave Points, Symmetry and Fractal Dimension features. Both size and shape are expressed by the Perimeter feature. Nuclear Texture is measured by finding the variance of the grey scale intensities in the component pixels. The mean value, worst (mean of the three largest values), and standard error of each feature were computed for each image, resulting in a total of thirty features.

In both our machine learning and statistical analyses, the accuracy of correctly classifying samples as benign or malignant is determined by ten-fold cross-validation ⁷.

Diagnostic classification procedure, MSM-T

The classification procedure is a variant on the Multisurface Method (MSM) ^{8,9} known as MSM-Tree (MSM-T) ^{10,11}. This method uses linear programming iteratively to place a series of separating planes in the feature space of the samples. If the benign and malignant sets can be separated by a single plane, the first plane will be so placed between them. If the sets are not linearly separable, MSM-T constructs a plane that minimizes an average distance of misclassified points. Depending on the separation accuracy attained, the procedure is recursively repeated on the two regions generated by each plane until satisfactory separation is achieved, i.e. each of the final regions contains mostly points of one category. The classifier thus obtained is then used as a decision tree to categorize new cases. As is often the case, the classifier's performance on unseen data is improved by using only a subset of the input features, and a small number of planes. In addition to providing a diagnosis, the program provides the probability that a new sample is malignant. This probability is estimated from the distance that the new point lies from the separating plane ².

Prognostic prediction procedure, RSA

We view prognostic prediction as a function estimation problem, where time of recurrence is predicted based on the input features (the thirty digital features, plus tumor size and positive lymph nodes). Our proposed solution to this estimation problem is the Recurrence Surface Approximation (RSA) method ¹². RSA uses linear programming to construct a predictive model, using both recurrent and non-recurrent cases, which predicts time to recur for new cases.

As in classification, it is important to choose the right subset of features to get the best generalization. In order to estimate both our accuracy and the number of features needed for prediction, we used leave-one-out cross validation, where a single case was set aside for testing a predictive model trained from the other cases. To select the best subset of features, we also set aside a tuning set ¹³, a randomly selected one fifth of the remaining cases. Hence, of the 190 cases, one was set aside for testing, 38 cases were placed in the tuning set and 151 cases remained in the training set (Figure 1). First, an RSA was constructed with the training set using all the features and the accuracy was tested against the tuning set. Testing was repeated as the features were removed one by one from the training set, each time removing the feature that contributed least to the predictive model, until only a single feature remained. The feature set which produced the best accuracy when tested against the tuning set was noted, and the features used at that point

were then used to generate an RSA with the combined tuning and training sets, 189 cases in all. The accuracy of this RSA was then tested against the case that had been initially set aside. This process was repeated until the accuracy of classifying each case had been determined, 190 times in all. The optimal number of features to be used (average 4.7) and the classification accuracy of digitally derived features versus lymph nodes and tumor size were determined in this manner.

One final RSA was constructed for prediction on new cancer patients. Using all the cases as a training set, features were eliminated until five remained. In addition to a predicted time of recurrence, this RSA is used to provide an estimated survival curve for new patients. A Kaplan-Meier plot¹⁴ is generated based on the observed recurrences for the 20% of patients having RSA-predicted times for distant recurrence the most similar to that of the new patient.

Statistical analyses were done with SAS¹⁵ software.

Results:

Diagnostic classification:

Independent samples t-test showed significant differences ($p < 0.001$) between benign and malignant values for all nuclear features except for the Mean of Fractal Dimension, Standard Error of Texture, Standard Error of Smoothness, Standard Error of Symmetry, and for Standard Error of Fractal Dimension.

A computationally intensive search revealed that Worst Area, Mean Texture and Worst Smoothness gave the most accurate three-feature, single plane classification separation. Seven benign and seven malignant FNAs were misclassified when MSM-T was used to classify with cross validation (Table 1). This indicated that classification of future samples would be correct 97% of the time. In practice, 118 consecutive, new samples were correctly classified. The Xcyt estimated probability of malignancy for these samples is shown as Figure 2.

Prognostic feature analysis for distant disease recurrence:

In a stepwise Cox regression analysis of prognostic features, a worst nuclear size feature was selected as the single most important feature in each of the five best two-feature models. After a nuclear size feature was selected, either the number of metastatic lymph nodes or tumor size was chosen as the second feature in each of the models. In the Cox proportional hazards analysis for the two-feature model, the p-value was 0.0001 for the largest nuclear area and was 0.0092 for the number of metastatic axillary lymph nodes. An analysis of deviance¹⁶ was performed in order to estimate the importance and interdependence of nuclear features relative to lymph node status (Table 2). For a single variable model, Worst Area is a better prognosticator than is lymph node status (Table 2, rows 1 and 2). The prognostic power of Worst Area plus lymph node status is

given in Table 2, row 3. Adjusting for Worst Area causes a large effect (Table 2, row 4), where as the effect of adjusting for lymph node status is less (Table 2, row 5). The adjusted numbers (Table 2, rows 4 and 5) are about the same as are the unadjusted ones (Table 2, rows 1 and 2 respectively), indicating that the contributions by Worst Area and lymph node status are independent of one another.

When machine learning with leave-one-out cross validation was used to select the optimal number of features for prognostic models, computer-derived nuclear Worst Radius was used 84.7% of the time, Worst Area 54.7%, Mean Radius 50.5%, Mean Perimeter 38.9%, Mean Fractal Dimension 21%,....., Node status 5.3%, and Tumor size 1.0% of the time.

Compared with the actual time for recurrence, the mean error of predicted times for recurrence with the nuclear features was 17.9 months and was 20.1 months with tumor size and lymph node status ($p=0.11$). The average number of features used during this process was 4.7.

Since the average number of features used was 4.7, the next step was to find the best five features to be used in a five-feature RSA for individual patient prognostic estimation. These were found to be Mean Radius, Mean Perimeter, Mean Fractal Dimension, Worst Radius, and Worst Area. The FNAs obtained from two patients are shown as Figures 3 and 4 and the Kaplan-Meier plot of the RSA data from these two patients, together with the

average for all 190 patients, is shown as Figure 5.

Discussion:

Nuclear feature analysis is better performed on cytologic FNA preparations than on the more commonly used histologic tissue samples. FNA cells are preserved intact whereas histologic processing cuts cells at various planes. Our nuclear size feature values are the same as those reported by Hutchinson et. al.¹⁷. However, our values for shape differ from those reported, probably due to different methods used for segmentation (i.e. designation of the nuclear boundary). Although absolute shape differences are small, they are statistically significant. The statistical significance arises from the variability in the measurements; 3% and 4% respectively for benign and malignant in our series versus 9% and 11% for that of Hutchinson et. al.¹⁷.

A size, a texture, and a shape feature were selected to give the most accurate diagnostic classification. The cross validated classification accuracy was 97.5%. These results are considerably better than the 89% accuracy based on digital cell analysis achieved in the literature¹⁷. Our improved accuracy apparently was achieved by our method of segmentation (snake) and through the use of shape and texture features not measured by others. Our cross validated performance parameters equal the

best reported for visual diagnosis ¹ and our prospective diagnostic accuracy is even better. We believe that our methods provide a basis for highly accurate computerized diagnostic systems for breast cytology. The estimated probability of malignancy given by the computer program compensates for diagnostic uncertainty inherent in cytologic diagnosis. The objective assessment of this uncertainty provides an objective basis for recommending open biopsy in questionable cases.

Some of the same nuclear features that are diagnostically important are components of visually assessed nuclear "grade". The prognostic value of nuclear grade of breast cancer has been well established since Black et al. ⁸ first described the relationship between prognosis and nuclear anaplasia in 1955. His grading system ¹⁹ was modified by Bloom and Richardson ²⁰ and subsequently many other investigators ^{20, 21, 22, 23, 24, 25, 26, 27} confirmed the relationship between nuclear anaplasia and prognosis. However, as with diagnosis, visual grading systems are subjective and are vulnerable to intra- and interobserver variation ²⁸. Despite this problem, recent studies continue to demonstrate the prognostic importance of visually assessed nuclear anaplasia ^{29, 30}.

Objective cell image analysis cell using computers has become increasingly sophisticated during the past 30 years ³¹. The results of computer-based analyses are reproducible and correlate closely with visual assessments ³². With the use of

such techniques, larger nuclear size was shown to be associated with a poorer prognosis ^{28,33,34,35}. In addition to size, computerized digital image analysis makes possible the measurement of a variety of nuclear shape ^{3,36} and texture features. Komitowski and Janson ³⁷ achieved 85% prognostic accuracy in 60 breast cancer patients with digital image analysis. They found nuclear size and nuclear chromatin structure features to be strongly prognostic. Others found variation in nuclear size, as reflected in the standard deviation of nuclear-size features, to be prognostically unfavorable ^{33,34,38}. A large trial is underway evaluating morphometry (nuclear area and axes ratio) relative to other prognostic factors ³⁹. In contrast to the segmentation methods used in other studies, our segmentation is automatically determined by the computer "snake" program.

We corroborate others observations that nuclear morphometric features provide prognostic information independent of that provided by tumor size and axillary lymph node involvement with metastatic disease ^{37,40}. Mittra and MacRae ⁴⁰ found in a meta-analysis that biological factors and tumor grade were not correlated with the clinical prognostic factors of axillary lymph node status and tumor size. In the Nottingham index, grade emerged as prognostically more powerful than tumor size or lymph-node status and was the only prognostically significant factor on multivariate analysis ²⁹.

We found that objectively and accurately assessed nuclear features are better prognostic indicators than are features, such as tumor size and lymph node status. Should others confirm our findings, patients can be spared axillary surgery for prognostic purposes. Not only would the magnitude of breast surgery be reduced, but the 20% incidence of arm lymphedema and susceptibility to infection following axillary dissection^{41,42} would be avoided. We conclude that computer-generated nuclear features are diagnostically important, and that particularly nuclear size features, are prognostically more important than are tumor size, and lymph node status. The computer program described in this paper provides the basis for improving FNA breast mass diagnosis and determining prognosis from computer-generated nuclear features.

References:

1. Giard RWM, Hermans J: The value of aspiration cytologic examination of the breast. A statistical review of the medical literature. *Cancer* 1992;69:2104-2110.
2. Wolberg WH, Street WN, Mangasarian OL: Machine learning techniques to diagnose breast cancer from image-processed nuclear features of fine needle aspirates. *Cancer Letters* 1994;77:163-171.
3. Street WN, Wolberg WH, Mangasarian OL: Nuclear feature extraction for breast tumor diagnosis. *Proceedings IS&T/SPIE International Symposium on Electronic Imaging* 1993;1905:861-870.
4. Layfield L, Chrischilles E, Cohen M, Bottles K: The Palpable Breast Nodule - A Cost Effective Analysis of Alternate Diagnostic Approaches. *Cancer* 1993;72:1642-1651.
5. Kass M, Witkin A, Terzopoulos D: Snakes: Active contour models. *Proc First Int Conf on Computer Vision* 1987;259-269.
6. Williams DJ, Shah M: A fast algorithm for active contours, in *Proc. Third Int. Conf. on Computer Vision*. Osaka, Japan, 1990:592-595.

7. Stone M: Cross-validatory choice and assessment of statistical predictions. *Journal of the Royal Statistical Society* 1974;36:111-147.

8. Mangasarian OL: Multi-surface method of pattern separation. *IEEE Trans on information theory* 1968;IT-14:801-807.

9. Mangasarian OL, Setiono R, Wolberg WH: Pattern Recognition via Linear Programming: Theory and Application to Medical Diagnosis, in Coleman TF, Li Y (eds): *Large-Scale Numerical Optimization*. Philadelphia, Pa, SIAM; 1990:22-30.

10. Bennett KP: Decision Tree Construction via Linear Programming, in Evans M (ed): *Proceedings of the 4th Midwest Artificial Intelligence and Cognitive Science Society Conference*. 1992:97-101.

11. Mangasarian OL: Mathematical programming in neural networks. *ORSA Journal on Computing* 1993;5:349-360.

12. Mangasarian OL, Street WN, Wolberg WH: Breast cancer diagnosis and prognosis via linear programming. *University of Wisconsin, Computer Sciences Department, Mathematical Programming Technical Report 94-10* 1994.

13. Lang K, Waibel A, Hinton G: A time-delay neural network architecture for isolated word recognition. *Neural Networks* 1990;3:23-43.
14. Kaplan EL, Meier P: Nonparametric estimation from incomplete observations. *J Am Statist Assoc* 1958;53:457-481.
15. *SAS/STAT User's Guide, Version 6*, Cary, NC, SAS Institute Inc. 1989.
16. McCullagh P, Nelder JA: McCullagh P, Nelder JA (eds): *Generalized Linear Models*. London, Chapman Hall; 1983.
17. Hutchinson ML, Isenstein LM, Zahniser DJ: High-resolution and contextual analysis for the diagnosis of fine needle aspirates of breast. *Analy Quant Cytol and Hist* 1991;13:351-355.
18. Black MM, Opler SR, Speer FD: Survival in breast cancer cases in relation to the structure of the primary tumor and regional lymph nodes. *Surg Gynecol Obstet* 1955;100:543-551.
19. Black MM, Speer FD: Nuclear structure in cancer tissues. *Surg Gynecol Obstet* 1957;105:97-102.

20. Bloom H, Richardson W: Histological grading and prognosis in breast cancer. *Br J Cancer* 1957;19:359-377.

21. Fisher ER, Redmond C, Fisher B, Bass G: Pathologic findings from the National Surgical Adjuvant Breast and Bowel Projects (NSABP). Prognostic discriminants for 8_year survival for node-negative invasive breast cancer patients. *Cancer* 1990;65(supp):2121-2128.

22. Henson DE, Ries L, Freedman LS, Carriaga M: Relationship among outcome, stage of disease, and histologic grade for 22,616 cases of breast cancer. *Cancer* 1991;68:2142-2149.

23. Le Doussal V, Tubiana-Hulin M, Friedman S, Hacene K, Spyrtos F, et al. Prognostic value of histologic grade nuclear components of Scraff-Bloom -Richardson (SCR): An improved score modification based on multivariate analysis of 1262 invasive ductal breast carcinomas. *Cancer* 1989;64:1914-1921.

24. Rank F, Dombernowsky P, Jespersin NCB, Pedersen BV, Keiding N: Histologic malignancy grading of invasive ductal breast carcinoma. *Cancer* 1987;60:1299-1305.

25. Todd JG, Dowle C, Williams MR, Elston CW, Ellis IO, et al. Confirmation of a prognostic index in primary breast cancer. *Br J*

Cancer 1987;56:489-492.

26. Wallgren A, Zajiecek J: The Prognostic Value of the Aspiration Biopsy Smear in Mammary Carcinoma. *Acta Cytologica* 1976;20:479-485.

27. Mouriquand J, Gozlan-Fior M, Villemain D, et al: Value of cytoprognostic classification in breast carcinomas. *J Clin Pathol* 1986;39:489-496.

28. Stenkvist B, Westman-Naeser S, Vegelius J, Holmquist J, Nordin B, et al. Analysis of reproducibility of subjective grading systems for breast carcinoma. *J Clin Path* 1979;32:979-985.

29. Galea MH, Blamey RW, Elston CE, Ellis IO: The Nottingham Prognostic Index in primary breast cancer. *Breast Cancer Res Treat* 1992;22:207-219.

30. Robinson IA, McKee G, Nicholson A, et al: Prognostic value of cytological grading of fine-needle aspirates from breast carcinomas. *Lancet* 1994;343:947-949.

31. Wied G, Bartels P, Bibbo M, Dytch H: Image Analysis in Quantitative Cytopathology and Histopathology. *Human Pathology*

1989;20:549-571.

32. VanDiest PJ, Risse EKJ, Schipper NW, Baak JPA: Comparison of light microscopic grading and morphometric features in cytological breast cancer specimens. *Path Res Pract* 1989;185:612-616.

33. Baak JPA, Kurver PHJ, Snoo-Niewlaat AJE, Graef S, Makkink B. Prognostic Indicators in Breast Cancer-Morphometric Methods. *Histopathology* 1982;6:327-339.

34. Baak JPA, VanDop H, Kurver PHJ, Hermans J: The Value of Morphometry to Classic Prognosticators in Breast Cancer. *Cancer* 1985;56:374-382.

35. Wittekind C, Schulte E: Computerized morphometric image analysis of cytologic nuclear parameters in breast cancer. *Analy Quant Cytol and Hist* 1987;9:480-484.

36. Partin AW, Walsh AC, Pitcock RV, Mohler JL, Epstein JI, Coffey DS: A Comparison of Nuclear Morphometry and Gleason Grade as a Predictor of Prognosis in Stage A2 Prostate Cancer: A Critical Analysis. *J Urol* 1989;142:1254-1258.

37. Komitowski D, Janson C: Quantitative features of chromatin

structure in the prognosis of breast cancer. *Cancer* 1990;65:2725-2730.

38. Pienta KJ, Coffey DS: Correlation of nuclear morphometry with progression of breast cancer. *Cancer* 1991;68:2012-2016.

39. Baak JPA, VanDiest PJ, Stroet-Van Galen C, Wisse-Brekelmans ECM, Matze-Cok E, Littooy JG: Data processing and analysis in the multicenter morphometric mammary carcinoma project. *Path Res Pract* 1989;185:657-663.

40. Mittra I, MacRae KD: A Meta-analysis of Reported Correlations between Prognostic Factors in Breast Cancer: Does Axillary Lymph Node Metastasis Represent Biology or Chronology? *Eur J Cancer* 1991;27:1574-1583.

41. Kissin MW, Querci della Rovere G, Easton D, Westbury G: Risk of lymphoedema following the treatment of breast cancer. *Br J Surg* 1986;73:580-584.

42. Aitken RJ, Gaze MN, Rodger A, Chetty U, Forrest APM: Arm morbidity within a trial of mastectomy and either nodal sample with selective radiotherapy or axillary clearance. *Br J Surg* 1989;76:568-571.

Table 1: Inductive machine learning classification: Predicted versus Confirmed Diagnosis.

	Malignant, Confirmed	Benign, Confirmed	Total
Malignant, Predicted	205	7	212
Benign, Predicted	7	350	357
Total	212	357	569

Table 2

Cox analysis of deviance (Partial likelihood) for independent prognostic contribution of the nuclear feature Worst Area relative to lymph node status.

	Feature	Deviance	p
1	Node status	5.68	0.017
2	Worst Area	14.21	0.0002
3	Worst Area and Node status	19.78	0.0001
4	Worst Area then Node status*	5.57	0.020
5	Node status then Worst Area**	14.11	0.0002

* Residual contribution of Node status after the contribution of Worst Area was removed.

** Residual contribution of Worst Area after the contribution of Node status was removed.

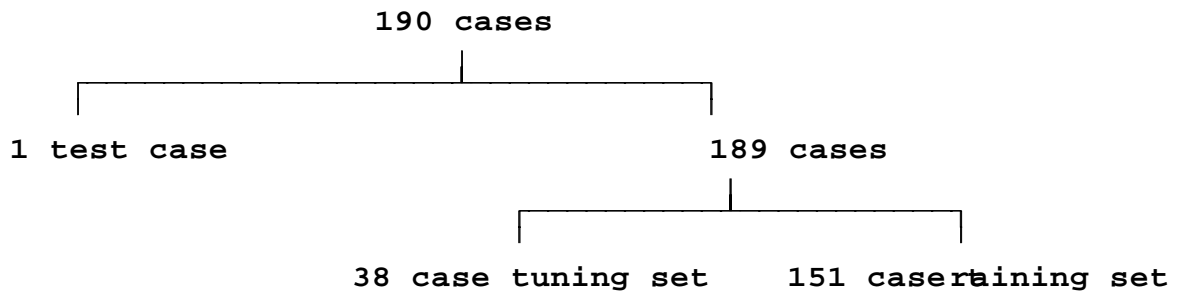


Figure 1: Splitting of the 190-patient data set into training, tuning and testing sets for prognostic purposes. See Prognostic Prediction Procedure section for details.

Figure 2: The Xcyt estimated probability of malignancy for 118 (87 benign (green bars) and 31 malignant (red bars)) consecutive, new FNAs.

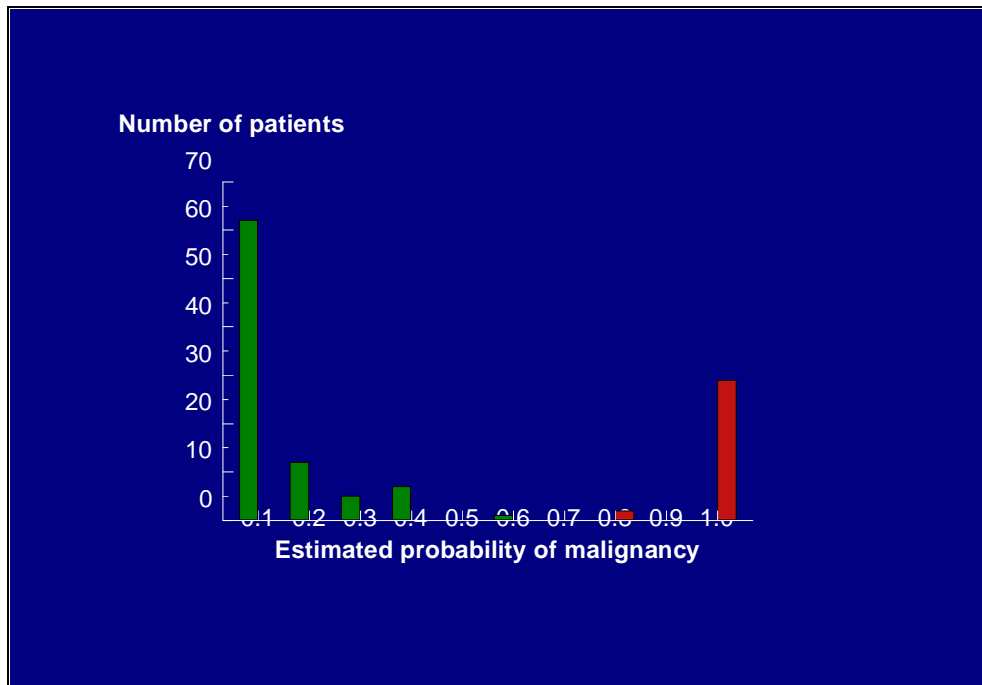


Figure 3: Photomicrograph (x 157.5) of the FNA obtained from patient J.S.

Figure 4: Photomicrograph (x 157.5) of the FNA obtained from patient D.L.

Figure 5: Kaplan-Meier survival curve derived from RSA analysis. Predicted survivals are given for:

- distant disease-free survival for all 190 patients,
- • - • - distant disease-free survival predicted for the patient, J.S., whose FNA is shown as Figure 3, and
- distant disease-free survival predicted the patient, D.L., whose FNA is shown as Figure 4.

